International Journal of Refrigeration

Viscosity of binary refrigerant mixtures of R32 + R1234yf and R32 + R1243zf

--Manuscript Draft--

Manuscript Number:	JIJR-D-20-00675R1
Article Type:	Research Paper
Keywords:	Viscosity, vibrating-wire viscometer, R32, R1234yf, R1243zf
Corresponding Author:	Xiaoxian Yang The University of Western Australia Perth, AUSTRALIA
First Author:	Xiaoxian Yang
Order of Authors:	Xiaoxian Yang
	Hangtao Liu
	Shi Hai Chen
	Dongchan Kim
	Fufang Yang
	Arash Arami-Niya
	Yuanyuan Duan
Abstract:	Viscosity measurements of six binary mixtures of R32+R1234yf and R32+R1243zf at different compositions were conducted in the homogenous liquid and gas phases with a vibrating-wire viscometer in the temperature range from (254 to 383) K and pressures from (1 to 8) MPa. The measurement system was verified with the measurements of pure carbon dioxide and R32 in homogenous liquid and gas phases. The relative combined expanded uncertainties (k = 2) in the experimental viscosity of the mixtures are generally from 3.2 % to 5.0 %. The measured viscosities agree with the calculations of the extended corresponding state model implemented in the software package REFPROP 10.0 within 10% and mainly within 5%. The parameters of the residual entropy scaling model incorporating cubic-plus-association equation of state (RES-CPA model) for the viscosity of pure R1243zf and binary R32 + R1243zf mixture were determined. The relative deviation of the measured viscosities from values calculated with the RES-CPA model is mainly within 5%.
Response to Reviewers:	Dear Dr. East: Thank you very much for your and the reviewers' comments to the manuscript of JIJR-D-20-00675. The comments are very valuable for improving this paper. We have carefully revised the manuscript according to the reviews' comments with details provided in the uploaded 'Response to Reviewers'. Please let us know if there is anything else needed. Best regards, Xiaoxian Yang, Hangtao Liu, Shi Hai Chen, Dongchan Kim, Fufang Yang, Arash Arami-Niya, Yuanyuan Duan

Viscosity of binary refrigerant mixtures of R32 + R1234yf and R32 + R1243zf

Xiaoxian Yang[1*], Hangtao Liu[2], Shi Hai Chen[1], Dongchan Kim[1], Fufang Yang[2,3], Arash Arami-Niya[1, 4], Yuanyuan Duan[2]

[1] Fluid Science & Resources Division, Department of Chemical Engineering, University of Western Australia, Crawley, WA 6009, Australia

[2] Key Laboratory for Thermal Science and Power Engineering of Ministry of Education, Beijing Key Laboratory for CO_2 Utilization and Reduction Technology, Tsinghua University, Beijing 100084, China

[3] Center for Energy Resources Engineering (CERE), Department of Chemical and Biochemical Engineering, Technical University of Denmark, 2800 Kgs. Lyngby, Denmark

[4] Discipline of Chemical Engineering, Western Australian School of Mines: Minerals, Energy and Chemical Engineering, Curtin University, GPO Box U1987, Perth, WA 6845, Australia

Abstract

Viscosity measurements of six binary mixtures of R32+R1234yf and R32+R1243zf at different compositions were conducted in the homogenous liquid and gas phases with a vibrating-wire viscometer in the temperature range from (254 to 383) K and pressures from (1 to 8) MPa. The measurement system was verified with the measurements of pure carbon dioxide and R32 in homogenous liquid and gas phases. The relative combined expanded uncertainties (k = 2) in the experimental viscosity of the mixtures are generally from 3.2 % to 5.0 %. The measured viscosities agree with the calculations of the extended corresponding state model implemented in the software package REFPROP 10.0 within 10% and mainly within 5%. The parameters of the residual entropy scaling model incorporating cubic-plus-association equation of state (RES-CPA model) for the viscosity of pure R1243zf and binary R32 + R1243zf mixture were determined. The relative deviation of the measured viscosities from values calculated with the RES-CPA model is mainly within 6% in the liquid phase and 10% in the gas phase.

Keywords: Viscosity, vibrating-wire viscometer, R32, R1234yf, R1243zf

*Corresponding author. *Email address:* xiaoxian.yang@uwa.edu.au. *Tel:* +61-4 1256 8598.

Nomenclature list

CPA	cubic-plus-association
ECS	extended corresponding states
EoS	equation of state
G	gas
GWP	global warming potential
HFC	hydrofluorocarbon
HFO	hydrofluoroolefin
L	liquid
R1234yf	2,3,3,3-Tetrafluoropropene
R1243zf	3,3,3-trifluoroprop-1-ene
R32	difluoromethane
RES	residual entropy scaling
SC	supercritical region
a_0, b, m, ε, β	parameters in the CPA EoS
A_1, A_3, A_4, A_0, and A_{-1}	coefficients in the univariate function of η^* with s^{res}
f	frequency
h	enthalpy
k	coverage factor
k_{ij}	binary interaction parameter
p	pressure
R	universal gas constant
s^{res}	residual entropy
T	temperature
u	standard uncertainty
U	expanded uncertainty
U_C	combined expanded uncertainty
V	induced voltage
x	mole fraction
η	viscosity
η^*	reduced viscosity
η_{calc}	viscosity calculated with the reference equations
η_{ECS}	viscosity calculated with the ECS model
η_{exp}	experimental viscosity
η_o	dilute gas viscosity
η_{RES}	viscosity calculated with the RES-CPA model
ξ	fluid-specific entropy scaling parameter
ρ	density
ρ_{EoS}	density calculated with EoS

1. Introduction

Due to the negligible ozone depletion potential and low global warming potential (GWP), hydrofluoroolefins (HFOs) are considered as the potential next generation of refrigerants (Calm, 2008; Pal et al., 2018). However, no pure refrigerant is ideal, each of which has one or more disadvantages: poor thermodynamic properties, toxicity, chemical instability, low to moderate flammability, or very high operating pressures (McLinden et al., 2014). For example, pure HFO-1234yf (2,3,3,3-Tetrafluoropropene, R1234yf) may not be suitable for certain applications due to its flammability (Zilio et al., 2011). Therefore, mixtures of HFOs, the traditional refrigerant hydrofluorocarbons (HFCs) and natural refrigerants are considered as practical alternatives. In our previous work (Yang et al., 2020), eight equimolar binaries and two multi-component mixtures containing HFOs, HFCs and CO_2 (natural refrigerant) were investigated. As a follow-up, binary systems of HFC-32 (difluoromethane, R32) + R1234yf and R32 + HFO-1243zf (3,3,3-trifluoroprop-1-ene, R1243zf) at various compositions were focused on in this work. R32 is currently used in residential and commercial air-conditioners in Japan, China and India as it has excellent heat transfer and pressure drop performance both in condensation and vaporisation. However R32 has relatively high GWP_{100} = 675, *i.e.*, a GWP index 675 times that of carbon dioxide based on a 100-year time frame. While the GWP_{100} of both R1234yf and R1243zf were reported less than 1 (Myhre et al., 2014).

Models of fluid viscosity are necessary for the design of a refrigeration system. A widely in use one for the prediction of mixtures' viscosity is the extended corresponding states (ECS) model (Chichester and Huber, 2008) implemented in the REFPROP 10.0 software package (Lemmon et al., 2018). In this semi-empirical model, the viscosity of a fluid is a function of temperature and density. The ECS model maps the viscosity of a reference fluid which has an accurate equation of state (EoS) and an accurate viscosity model onto the fluid of interest according to the correspondence of the residual Helmholtz energy and the compressibility factor. Recently, another modelling approach based on the residual entropy scaling (RES) law received increasing attentions and was verified in various real fluids (Bell, 2019, 2020; Liu et al., 2020; Taib and Trusler, 2020). According to the RES law, the dependence of viscosity on the thermodynamic state was reduced to a univariate function of the residual entropy for both pure fluids and mixtures in wide ranges of temperature and pressure. Since only a single variable is involved, far fewer experimental data

points would be required. We recently have applied the RES law incorporating the cubic-plus-association EoS (RES-CPA model) to calculate the viscosity of HFCs, HFOs, and their binary mixtures(Liu et al., 2020).

The accuracy of the models relies on the available experimental data that the parameters of the models are anchored to. The available viscosity data of the binary R32 + R1234yf mixture are rare, a summary of the selected literature is listed in Table 1, while there is no data of the binary R32 + R1243zf mixture reported in literature. To improve the current data situation, measurements were carried out for these two binary systems with R32 mole fraction of 0.25, 0.50 and 0.75, respectively, in the temperature range from (254 to 383) K and pressures from (1 to 8) MPa in the homogenous liquid and gas phases with a vibrating-wire viscometer.

Table 1. Selected literature with experimental viscosity data of the investigated mixture systems.

System	T/ K	p/MPa	x_1 range[a]	Author and Year
R32 + R1234yf	283 – 320	2.23-3.02	0.484 – 0.836	(Dang et al., 2015a)
R32 + R1234yf	278 – 338	0.10-0.11	0.354 – 0.687	(Dang et al., 2015b)
R32 + R1234yf	293 – 343	0.98-4.39	0.519 – 0.795	(Cui et al., 2016)

[a] Mole fraction of the first component in the "system" column.

2. Experimental

2.1. Experimental material

The pure fluid samples were provided by Coregas; they were used as received from the supplier without further gas analysis or purification. Detailed information of the pure fluid samples is summarized in Table 2. The investigated mixtures were prepared volumetrically in our laboratory with a detailed preparation procedure described previously (Al Ghafri et al., 2019). The composition information of the prepared mixtures is listed in Table 3. The expanded uncertainty (k = 2) in the composition of the mixture samples was estimated to be 0.028 mole fraction (Al Ghafri et al., 2019; Yang et al., 2020).

Table 2 Information of the pure fluid samples

ASHRAE Refrigerant Number	CAS Reg. No.	IUPAC name	Source	Purity/mole fraction

R32	75-10-5	Difluoromethane	Coregas	0.9999[a]
R1234yf	754-12-1	2,3,3,3-Tetrafluoropropene	Coregas	0.9999[a]
R1243zf	677-21-4	3,3,3-trifluoroprop-1-ene	Coregas	0.9999[a]
CO_2	124-38-9	Carbon Dioxide	Coregas	0.99995[b]

[a] The purity was given by the supplier. Impurity information was not provided by the supplier.

[b] Impurities (stated by supplier): $x(H_2O) \leq 7\times10^{-6}$, $x(O_2) \leq 1\times10^{-5}$, x(other C_mH_n) $\leq 5\times10^{-6}$, x(CO) $\leq 2\times10^{-6}$, where x denotes mole fraction.

Table 3 Information of the mixtures

Mixtures	Compositions/mole fraction			Expanded uncertainty (k = 2) /mole fraction
	R1243zf	R1234yf	R32	
Mix. 1	0.750	-	0.250	0.028
Mix. 2	0.250	-	0.750	0.028
Mix. 3	0.500	-	0.500	0.028
Mix. 4	-	0.750	0.250	0.028
Mix. 5	-	0.250	0.750	0.028
Mix. 6	-	0.500	0.500	0.028

2.2. Measurement

Viscosity measurements of the single-phase fluid were carried out with a doubly-clamped vibrating-wire viscometer. The measurement principle and experimental setup of the viscometer was explained in detail previously (Czubinski et al., 2018; Locke et al., 2015a; Locke et al., 2015b; Locke et al., 2014; Stanwix et al., 2014; Yang et al., 2020), especially in the latest publication[5]. In brief, a tungsten wire clamped at both end and immersed in the fluid sample was driven by passing a sinusoidal current through it, and the amplitude of the wire's displacement was monitored by measuring the electromagnetically induced voltage V through demodulation and subtraction of the drive signal. In an equilibrium measurement, the frequency f of the drive signal was stepped increased and then decreased with a span at least twice of the half-bandwidth and centered at the resonance frequency. The voltage across the wire V was recorded at each frequency f and the viscosity of the fluid was determined by regressing the (f, V) data[5]. The measurement system operates over the temperature range from (203.15 to 423.15) K and pressures up to 40 MPa with

expanded measurement uncertainties (k = 2) being 0.30 K in temperature, 4.2 kPa in pressure, and approximately 3.0 % in viscosity of pure fluids.

The measurement procedure was described in detailed previously as well (Yang et al., 2020). Here only further detail regarding how any phase transition (which would result in an inadvertent change in the composition) was avoided in the process of transitioning the sample in the measuring cell from a homogenous liquid to a homogenous gas is presented. The schematic diagrams of a measurement in the homogeneous liquid and gas phases are depicted in Figure 1 and Figure 2, respectively. The measurements commenced with the fluid in the liquid phase with the sample in the measuring cell in contact with the single-phase liquid within the inlet syringe pump, which was used to control the system pressure (see Figure 1). After the measurements in the liquid phase were complete, the liquid in the measuring cell was pressurized to at least 1 MPa higher than the critical pressure and then heated slowly with a rate less than 0.1 $K \cdot min^{-1}$ to a temperate at least 10 K higher than the critical temperature. When the fluid mixture had stabilized at the conditions of the supercritical state, the measuring cell was isolated from the inlet syringe pump (see Figure 2), and then the pressure of the fluid mixture was slowly reduced along an isotherm by slightly opening a needle valve between the measuring cell and an outlet syringe pump, which was filled with a fluid at a pressure kept 0.5 MPa below that of the fluid in the cell. When the designated cell pressure was reached, the isolating needle valve was closed. The measurements in the gas phase were carried out in a sequence of reducing density, which was achieved by the temperature control and the operation of the needle valve.

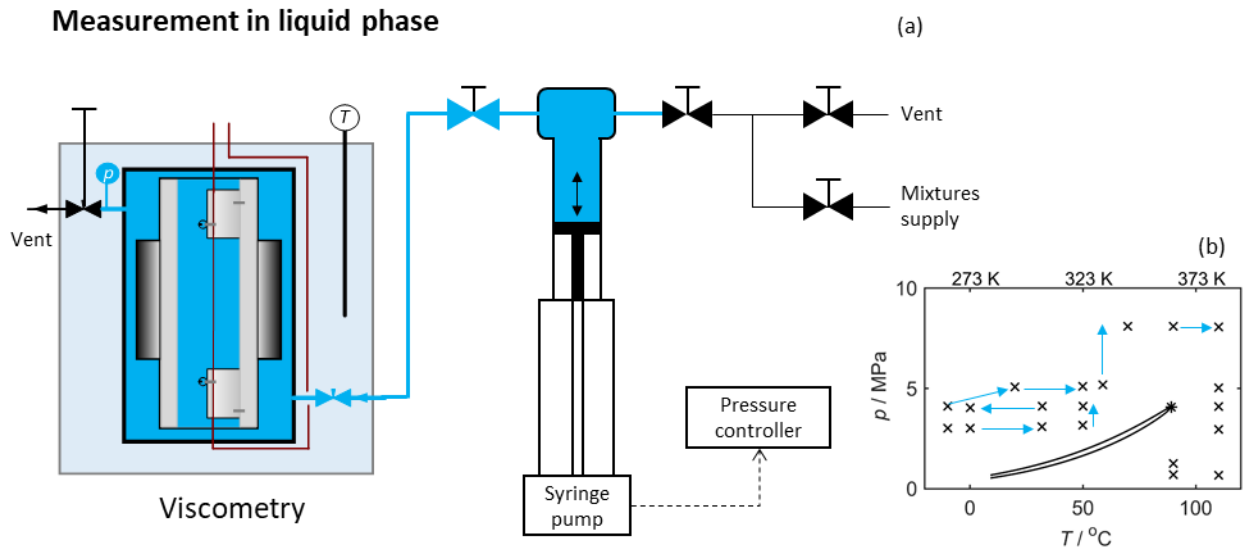

Figure 1. (a) The schematic diagram of the measurements in the liquid phase and in the supercritical region, (b) the pressure-temperature *pT* phase diagram of the exemplar (0.250 R32 + 0.750 R1234yf) mixture. ×, values measured in the present work; ✳, critical point; –, phase boundaries calculated with REFPROP 10(Lemmon et al., 2018). The arrows denote the key steps in the experimental procedure.

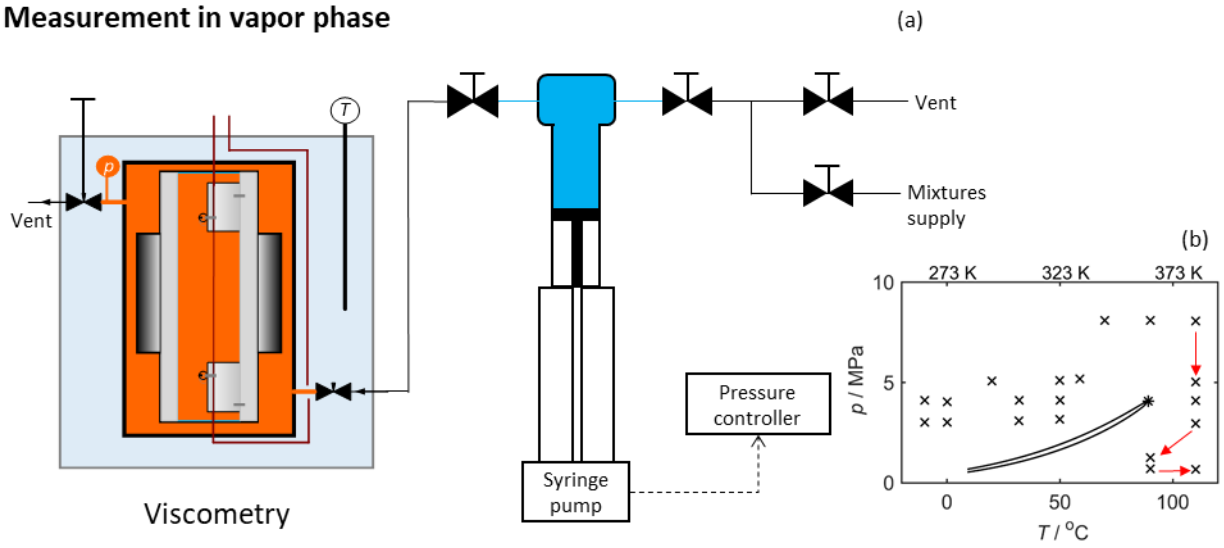

Figure 2. (a) The schematic diagram of the measurements in the gas phase, and (b) the pressure-temperature *pT* phase diagram of the exemplar (0.250 R32 + 0.750 R1234yf) mixture. ×, values measured in the present work; ✳, critical point; –, phase boundaries calculated with REFPROP 10 (Lemmon et al., 2018). The arrows denote the key steps in the experimental procedure.

2.3 Uncertainty analysis

The uncertainty of the experimental viscosity was estimated following the "Guide to the Expression of Uncertainty in Measurement" (GUM) (ISO/IEC Guide 98-3, International Organization for Standardization, Geneva, 2008). Unless otherwise stated, all uncertainties in this work are expanded uncertainties (k = 2) with a confidence level of 95 %. The uncertainties associated with the calculations (including calibration, data correlation and scatter), measurements (including temperature, pressure, frequency and voltage), parameters (mainly the calculated density using an EoS) and the composition of the mixture were taken into consideration. A detailed uncertainty analysis was given in our previous work (Yang et al., 2020). A budget for the combined uncertainty in the viscosity $U_C(\eta)$ is listed in Table 4 with the measurement of the (0.500 R32 + 0.500 R1234yf) mixture at T = 293.71 K, p = 5.033 MPa (liquid phase) and at T = 373.18 K, p = 6.014 MPa (in the supercritical region) taken as example conditions. The calibration together with the scatter of repeated measurements are the dominant factors contributing to the overall uncertainty. Across all conditions measured, the relative combined expanded uncertainties (k = 2) in the experimental viscosity of the mixtures are generally from 3.2 % to 5.0 %. Viscosity values in the gas phase generally have higher relative uncertainty than in the liquid phase; reasons are the higher relative uncertainty in pressure and the larger scatter in the gas-phase measurements. The relative uncertainty of viscosity measured in the vicinity of the critical point is as high as 7.5 % mainly attributed to the uncertainty of the mixture composition (see Table 4).

Table 4 Uncertainty budget for the viscosity. As examples, the measurements of binary mixture (0.500 R32 + 0.500 R1234yf) at T = 293.71 K, p = 5.033 MPa (liquid phase) and at T = 373.18 K, p = 6.014 MPa (in the supercritical region) were taken.[a]

Source	Uncertainty U	Contribution to $U_C(\eta)/\eta$
Calculations		
Calibration[b]	3.00 %	3.00 %
Data correlation[c]	1.00 %	1.00 %
Scatter of replicate measurements	1.82 % | 0.21 %	1.82 % | 0.21 %
Combined uncertainty attributed to calculations		3.65 % | 3.17 %
Measurements		
Temperature	320 mK	0.07 % | 1.20 %
Pressure	42 kPa	< 0.01 % | 0.19 %

Frequency f	$10 \cdot 10^{-6} \cdot f$	< 0.01 % | < 0.01 %
Induced voltage V	$0.01 \cdot V$	0.03 % | 0.01 %
Combined uncertainty attributed to measurements		0.07 % | 1.22 %
Parameters and Constants		
Density of the fluid mixture ρ [d]	$0.02 \cdot \rho$	0.28 %
Density of the Tungsten wire (19256 kg·m^{-3})	30 kg·m^{-3}	0.08 %
Combined uncertainty attributed to parameters		0.29 %
Compositions		
x_{prepare}	0.028 mol. frac.	0.23 % | 6.58 %
Combined uncertainty attributed to composition		0.23 % | 6.58 %
Summary: Combined uncertainty for mixtures $U_C(\eta)/\eta$		3.67 % | 7.41 %

[a] The values v_1 and v_2 presented in the format v_1 | v_2 are that for the example in the liquid phase and that for the example in the supercritical region, respectively. Three significant digits are used to express uncertainty in order to show more information for the small uncertainty contribution of certainty sources.

[b] The uncertainty attributed to the calibration is based on the calibration measurements with pure CO_2 in our latest publication (Yang et al., 2020).

[c] The correlation the (f, V) data to obtain viscosity.

[d] Estimated according to the references equation of state implemented in the REFPROP 10.0 (Lemmon et al., 2018).

3. Modelling

The residual entropy scaling law incorporating cubic-plus-association EoS (RES-CPA model) were developed for HFCs, HFOs and their binary mixtures previously (Liu et al., 2020). The relation between the reduced viscosity η^* and residual entropy s^{res} was described through a univariate function

$$\ln \eta^* = \ln \frac{\eta}{\eta^{\text{o}}} = A_1 \cdot \frac{s^{\text{res}}}{\xi R} + A_3 \cdot \left(\frac{s^{\text{res}}}{\xi R} \right)^3 + A_4 \cdot \left(\frac{s^{\text{res}}}{\xi R} \right)^4 + A_{-1} \cdot \left(\frac{1}{A_0 + s^{\text{res}} / \xi R} - \frac{1}{A_0} \right) \quad (1)$$

where η was the real fluid viscosity, η^{o} was the dilute gas viscosity, R is the universal gas constant, A_1, A_3, A_4, A_0, and A_{-1} were a set of universal coefficients for all the investigated HFCs and HFOs which were determined using the viscosity data of R134a in our previous work (Liu et al., 2020), and ξ was a fluid-specific parameter to compensate for the slight differences of the property of other HFCs/HFOs from R134a. The dilute gas viscosity, η^{o}, was obtained by Chapman-Enskog theory and taken as a baseline of the reduced viscosity η^* in RES model for a good scaling

performance. The residual entropy, s^{res}, as a function of T and ρ, was derived from CPA EoS, a model that was adapted for the thermodynamic properties of HFCs and HFOs, accounting for the effect of weak hydrogen bonding among HFC/HFO molecules and thus representing the thermodynamic properties accurately in both the gas and liquid phases.

For the binary mixtures, the van der Waals mixing rules and the Elliot combining rule of the CPA EoS, and the kinetic theory for the dilute gas mixture viscosity were used accounting for the interactions between the mixture components. The parameter ξ for the mixtures were obtained through the mole fraction weighted average of ξ for the components. The only mixture-specific adjustable parameter was the binary interaction parameter, k_{ij}, in the van der Waals mixing rules. Thus, the expression developed with pure fluid data was extended to the binary mixtures directly.

4. Results

4.1. Verification

The measurement system was calibrated and verified in our previous work (Yang et al., 2020) and is verified again in this work with the measurements of pure R32 and pure CO_2 in both liquid and gas phases. The relative deviations of the experimental viscosity from values calculated with the reference equations (CO_2 (Laesecke and Muzny, 2017) and R32 (Huber et al., 2003)) implemented in REFPROP 10.0 (Lemmon et al., 2018) are illustrated in Figure 3. The densities in Figure 3 were calculated with the reference EoS (CO_2 (Span and Wagner, 1996) and R32 (Outcalt and McLinden, 1995)). Comparisons with the best-selected experimental data in literature collected in the NIST TDE database (Frenkel et al., 2005) are illustrated in Figure 3, as well. In general, the relative deviations of our experimental values from the reference equations are within the scatter of the literature data. Although the data of CO_2 in the gas phase slightly negatively deviate from the best-selected literature dataset, they still agree with the reference equation within 3.0 %, which is the estimated uncertainty of our measurement for pure fluids.

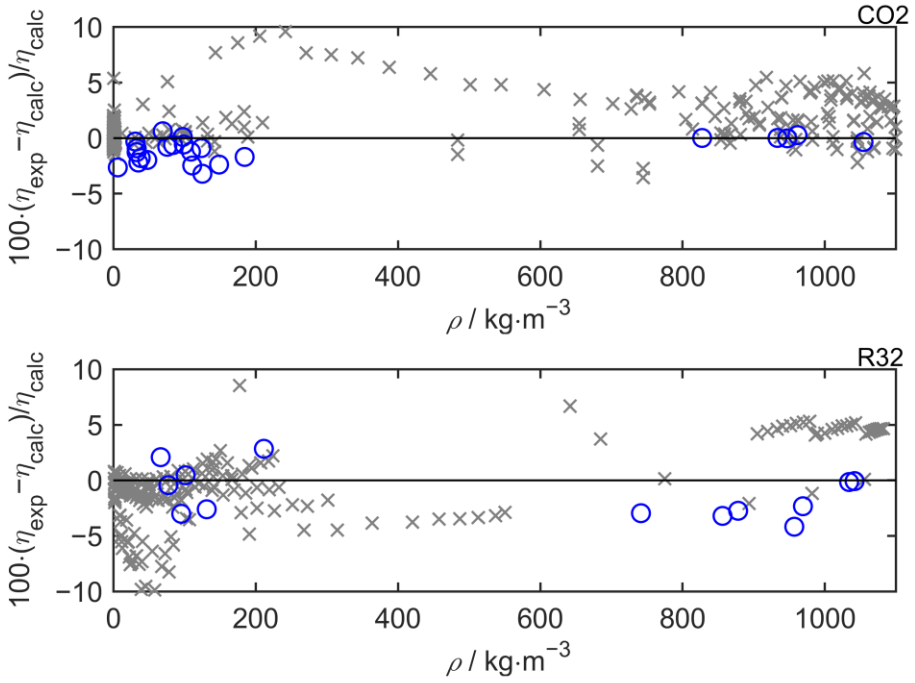

Figure 3. The relative deviations of the experimental viscosities η_{exp} from values η_{calc} calculated with the reference equations (CO_2 (Laesecke and Muzny, 2017), R32 (Huber et al., 2003)) implemented in REFPROP 10.0 (Lemmon et al., 2018). ○, data measured in this work; ×, data in literature as obtained from the NIST TDE database (Frenkel et al., 2005).

4.2. Measurement results

The experimental (T, p, η) data of the six binary mixtures are listed in Table 5 together with the calculated density ρ_{EoS} and the relative combined expanded uncertainty in viscosity $U_C(\eta)/\eta$. The density of the mixtures ρ_{EoS} was calculated using the measured temperature and pressure with the reference Helmholtz EoS implemented in the REFPROP 10.0 (Lemmon et al., 2018). The density value is listed as it is an important parameter used in determining viscosity (Yang et al., 2020). The relative deviations of the experimental viscosity from the values calculated with the ECS model (Chichester and Huber, 2008) as implemented in the REFPROP 10.0 are depicted in Figure 4 and Figure 5 for R32 + R1234yf and R32 + R1243zf, respectively. The relative deviations are within 10% and generally within 5%. No obvious systematic deviation related to density, pressure, temperature or composition was observed. Comparisons with the best-selected data in literature summarized in Table 1 are depicted in Figure 6. The relative deviations of the experimental values

of R32 + R1234yf mixtures from the ECS model(Chichester and Huber, 2008) are within the scatter of the literature data.

Table 5. The experimental viscosity η of the mixtures and its relative combined expanded uncertainty ($k = 2$) $U_C(\eta)/\eta$.[a]

T /K	p /MPa	ρ_{EoS} /(kg·m^{-3})	η /(μPa·s)	100 $U_C(\eta)/\eta$	Status[b]
		0.50 R32+0.50 R1234yf			
254.14	3.973	1198.1	208.91	3.9	L
264.09	4.982	1171.1	189.92	3.5	L
273.30	4.994	1141.8	177.78	3.8	L
293.09	4.009	1067.1	138.53	3.9	L
293.71	5.033	1071.1	146.30	3.7	L
294.94	6.037	1072.6	141.90	4.1	L
313.17	4.016	982.3	110.13	3.3	L
313.17	5.006	992.1	113.30	3.3	L
313.17	5.988	1001.0	116.50	3.4	L
313.17	8.011	1017.4	122.04	3.3	L
323.15	1.788	74.5	12.82	4.3	G
333.15	1.933	76.8	13.35	4.2	G
333.16	5.010	888.6	87.08	3.5	L
333.16	4.989	888.2	86.91	3.3	L
333.16	5.994	905.2	90.19	3.4	L
333.16	8.060	933.2	96.95	3.3	L
343.15	2.062	78.1	13.88	4.1	G
353.16	2.191	79.3	14.49	4.1	G
353.16	3.454	161.4	16.48	5.0	G
353.19	8.087	827.0	75.59	3.3	SC
363.17	2.973	112.9	15.90	4.3	G
363.16	3.769	166.3	17.35	4.8	G
373.17	4.128	173.4	18.11	4.6	G
373.17	5.943	420.7	31.61	7.5	SC
373.18	6.015	436.3	32.87	7.4	SC

T /K	p /MPa	ρ_{EoS} /(kg·m^{-3})	η /(μPa·s)	100 $U_C(\eta)/\eta$	Status [b]
373.18	8.088	674.8	55.01	3.7	SC
		0.75 R32+0.25 R1234yf			
263.34	4.923	1141.8	185.41	3.4	L
273.31	4.037	1105.8	163.34	3.4	L
304.04	3.088	980.3	111.73	4.2	L
302.97	5.019	1000.0	117.06	4.8	L
313.16	2.998	933.8	98.84	3.3	L
313.16	4.076	945.5	101.99	3.3	L
313.16	4.994	954.5	104.55	3.3	L
313.16	8.043	979.7	112.01	4.7	L
323.16	1.834	59.3	13.38	4.4	G
323.11	4.056	890.2	87.88	3.3	L
333.15	8.106	889.1	87.67	3.3	L
343.15	2.076	61.1	14.36	4.3	G
343.16	3.130	109.8	15.06	4.8	G
353.17	3.662	128.2	16.07	4.9	G
353.16	8.105	764.9	66.31	3.3	SC
363.16	2.153	57.3	15.58	4.2	G
363.17	3.185	95.0	16.14	4.5	G
363.12	3.866	126.6	16.84	4.9	G
373.17	4.114	127.5	17.34	4.6	G
373.18	8.067	544.2	41.24	4.6	SC
		0.25 R32+0.75 R1234yf			
263.31	3.019	1193.2	211.93	3.5	L
263.29	4.117	1197.5	215.17	3.4	L
273.32	3.011	1161.6	190.34	3.5	L
273.30	4.045	1166.3	192.09	3.4	L
293.11	5.084	1106.1	156.92	3.9	L
304.99	3.085	1047.7	134.52	4.2	L
305.16	4.121	1055.4	135.02	4.6	L
323.15	3.170	965.7	105.25	3.3	L

T /K	p /MPa	ρ_{EoS} /(kg·m^{-3})	η /(μPa·s)	100 $U_C(\eta)/\eta$	Status [b]
323.16	4.113	978.0	108.43	3.3	L
323.14	5.106	989.6	112.09	3.3	L
331.93	5.175	949.2	100.66	4.7	L
342.95	8.092	936.9	97.24	3.5	L
363.19	0.704	24.6	15.16	3.6	G
363.18	1.264	47.2	15.19	3.7	G
363.18	8.100	835.2	77.45	3.5	L
383.20	0.677	22.1	16.11	3.8	G
383.20	2.953	123.2	17.36	4.1	G
383.20	4.105	209.1	20.49	3.8	G
383.20	5.027	329.3	27.31	3.6	SC
383.20	8.068	700.4	58.30	3.3	SC
		0.50 R32+0.50 R1243zf			
299.79	4.140	966.0	127.91	3.2	L
300.94	3.132	955.1	123.64	3.2	L
303.94	4.073	950.5	121.59	3.2	L
306.44	4.099	941.3	118.15	3.3	L
306.48	6.090	954.7	123.10	3.3	L
313.15	3.204	906.7	107.02	3.3	L
313.08	4.112	915.2	108.89	3.2	L
313.16	6.041	930.3	114.50	3.4	L
313.16	8.106	944.6	118.66	3.3	L
323.16	4.065	870.5	98.14	3.3	L
323.16	6.049	891.2	103.14	3.2	L
323.16	8.105	908.9	107.59	3.2	L
333.17	4.049	818.0	85.94	3.2	L
333.17	6.057	847.3	91.87	3.3	L
343.18	1.990	66.8	13.77	3.9	G
343.18	6.055	795.9	81.22	3.3	L
343.19	8.098	826.6	86.83	3.3	L
353.19	2.043	64.9	14.31	3.8	G

T /K	p /MPa	ρ_{EoS} /(kg·m^{-3})	η /(μPa·s)	100 $U_C(\eta)/\eta$	Status [b]
363.20	2.076	62.5	14.95	3.8	G
363.20	2.295	71.1	15.13	3.8	G
363.20	8.070	718.8	68.49	3.5	SC
373.22	2.081	59.6	15.24	3.7	G
373.19	2.454	73.2	15.58	3.8	G
383.23	3.014	90.5	16.37	3.9	G
383.23	3.902	130.6	17.59	4.1	G
383.23	6.093	319.1	30.25	6.5	SC
383.22	8.022	554.1	50.14	4.2	SC
		0.75 R32+0.25 R1243zf			
303.37	3.016	938.6	110.53	4.3	L
303.39	4.013	945.8	113.74	4.2	L
303.41	5.005	952.5	116.15	4.3	L
312.78	3.008	895.4	98.72	3.2	L
312.78	4.006	905.0	101.43	3.2	L
312.79	5.002	913.7	103.21	3.3	L
312.79	6.002	921.8	106.44	3.3	L
322.65	4.004	855.3	89.47	3.2	L
322.73	5.004	867.0	91.72	3.3	L
322.68	6.002	878.1	94.50	3.2	L
332.59	5.002	811.4	80.55	3.2	L
332.59	6.003	827.2	83.91	3.2	L
342.52	1.712	45.1	13.47	3.9	G
352.52	1.804	45.7	14.01	4.1	G
352.51	2.579	71.7	14.47	4.0	G
362.51	1.895	46.2	14.73	3.8	G
362.51	2.914	79.2	15.28	4.1	G
372.54	2.004	47.2	15.20	3.8	G
372.54	2.250	54.1	15.34	3.9	G
382.58	2.563	60.3	15.84	3.9	G
		0.25 R32+0.75 R1243zf			

T /K	p /MPa	ρ_{EoS} /(kg·m^{-3})	η /(μPa·s)	100 $U_C(\eta)/\eta$	Status [b]
303.14	3.034	960.6	128.09	3.6	L
303.04	4.029	967.3	129.92	3.6	L
303.19	5.056	972.9	132.60	3.3	L
313.09	2.735	922.8	113.38	3.2	L
313.09	4.041	933.3	116.63	3.3	L
313.15	4.033	933.0	116.78	3.2	L
313.14	5.046	940.5	119.59	3.2	L
313.15	6.059	947.4	122.00	3.3	L
323.14	4.038	895.7	104.21	3.2	L
323.14	5.040	904.9	106.65	3.3	L
323.14	6.060	913.5	109.40	3.3	L
333.13	5.031	865.5	96.39	3.2	L
333.13	6.084	876.8	99.42	3.3	L
333.13	8.078	895.1	104.19	3.2	L
343.13	1.457	53.8	12.98	3.7	G
353.14	1.529	54.0	13.50	3.7	G
353.13	8.104	819.4	84.67	3.2	L
363.14	1.599	54.2	14.09	3.7	G
363.13	3.122	146.5	17.29	5.0	G
373.15	1.668	54.3	14.48	3.7	G
373.14	3.231	137.2	16.94	4.5	G
373.14	8.050	723.4	68.40	3.3	SC
383.14	2.082	68.0	15.14	4.1	G
383.14	2.468	84.6	15.50	3.8	G
383.14	3.022	112.4	16.33	4.4	G

[a] The expanded uncertainties (k = 2) of the measurements are 0.32 K for temperature T (ITS-90) and 0.042 MPa for pressure p; ρ_{EoS} is the density calculated with the Helmholtz equations of state for these mixtures implemented in the REFPROP 10.0 (Lemmon et al., 2018).

[b] G: gas phase; L: liquid phase; and SC: supercritical region.

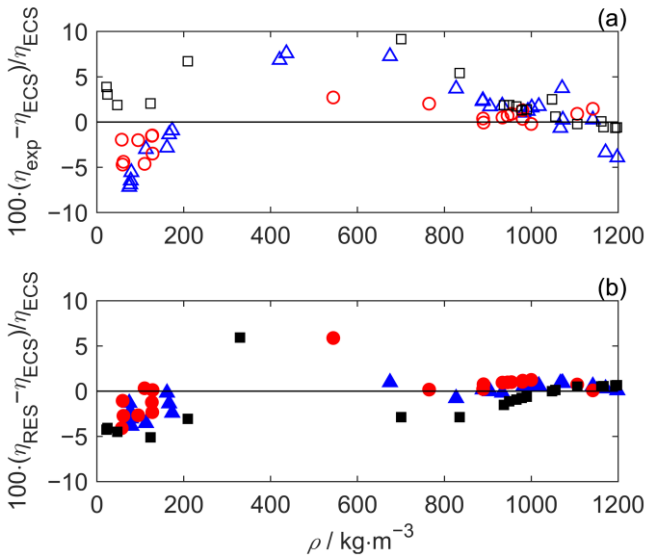

Figure 4. (a) Relative deviations of the experimental viscosities η_{exp} of R32 + R1234yf from values η_{ECS} calculated with the ECS model (Chichester and Huber, 2008) implemented in REFPROP 10.0 (Lemmon et al., 2018) plotted versus density ρ. (b) Relative deviations of the viscosities η_{RES} calculated with the RES-CPA model from η_{ECS}. Symbols: mixtures with R32 mole fraction of □■ 0.25, △▲ 0.50, and ○● 0.75.

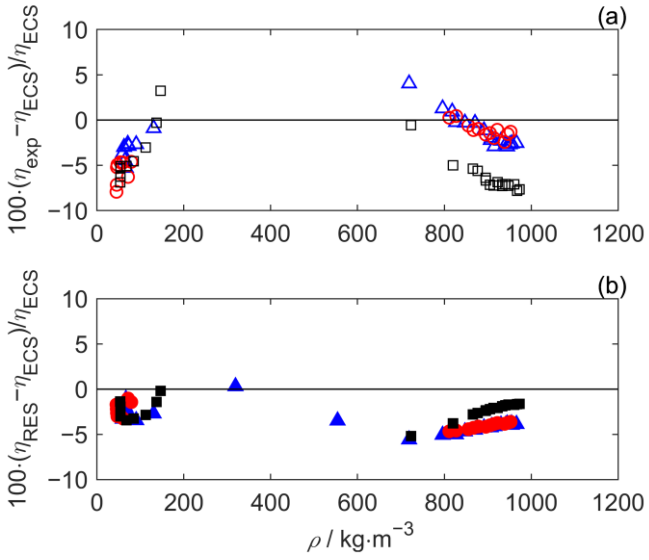

Figure 5. (a) Relative deviations of the experimental viscosities η_{exp} of R32 + R1243zf from values η_{ECS} calculated with the ECS model (Chichester and Huber, 2008) implemented in REFPROP 10.0 (Lemmon et al., 2018) plotted versus density ρ. (b) Relative deviations of the viscosities η_{RES} calculated with the RES-CPA model from η_{ECS}. Symbols: mixtures with R32 mole fraction of □■ 0.25, △▲ 0.50, and ○● 0.75.

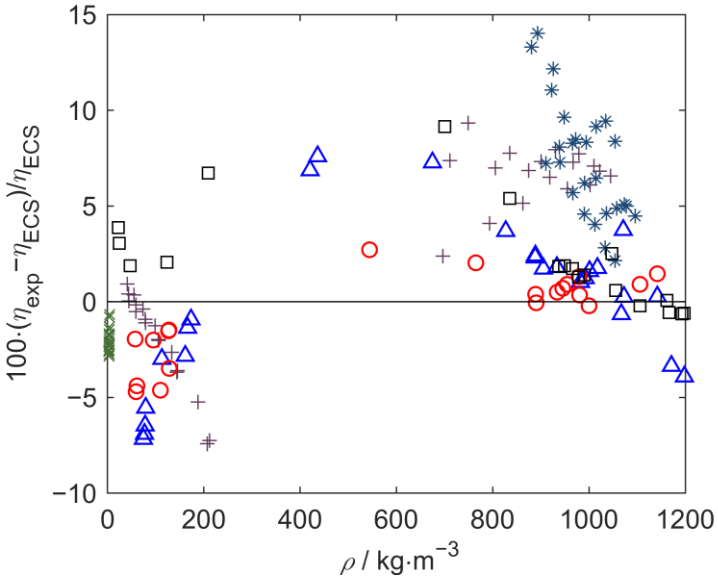

Figure 6. Relative deviations of the experimental viscosities η_{exp} of R32 + R1234yf from values η_{ECS} calculated with the ECS model (Chichester and Huber, 2008) implemented in REFPROP 10.0 (Lemmon et al., 2018). Symbols: this work with R32 mole fractions of □ 0.25, △0.50 and ○ 0.75; literature of + Cui et al (Cui et al., 2016), × Dang et al (Dang et al., 2015b), ✳ Dang et al (Dang et al., 2015a).

4.3 Comparison with RES-CPA model

The parameters of the RES-CPA model for pure R32, pure R1234yf and their binary interaction parameter (k_{ij} = 0.0549) were obtained from Yang et al (Yang et al., 2019) and Liu et al (Liu et al., 2020). The parameters of the CPA EoS for pure R1243zf (see Table 6) was obtained in this work anchoring to the vapor pressure (Brown et al., 2013; Higashi et al., 2018), liquid density (Di Nicola et al., 2013; Higashi and Sakoda, 2018) and vapor density (Di Nicola et al., 2013) data using a genetic multi-objective optimization algorithm. The binary interaction parameter for R32 + R1243zf (k_{ij} = 0.1150) was anchored to the phase boundary curves obtained from REFPROP 10.0 (Lemmon et al., 2018). In our previous work (Liu et al., 2020), the parameter ξ was determined for each pure fluid by fitting to the experimental viscosity data. However, no experimental viscosity data of pure R1243zf can be found from literature. Noticing that ξ of the mixture is the mole weighted average of ξ of the components, we fitted ξ for (0.75 R32+0.25 R1243zf), (0.50 R32+0.50 R1243zf) and (0.25 R32+0.75 R1243zf) separately, and then extrapolate to pure R1243zf. The parameters of the RES-CPA model for the pure R1243zf are listed in Table 6. The

relative deviation of the measured viscosities from values calculated with the RES-CPA model is generally within 6% in the liquid phase and 10% in the gas phase as illustrated in Figure 7. The comparisons between the RES-CPA model and ECS model are depicted in Figure 4 and Figure 5 for R32 + R1234yf and R32 + R1243zf, respectively. Compared to the ECS model, there are fewer adjustable parameters in the RES-CPA model, while the RES-CPA model yields similar agreement with the experimental data. Both models have significantly larger deviation (higher than 10%) from the experimental data in the vicinity of the critical point.

Table 6. Parameters of RES-CPA model for pure fluids

Fluid	CPA EoS					entropy scaling
	b/(m^3·mol^{-1})	a_0/(Pa·m^6·mol^{-1})	m	ε	β	ξ
R1243zf	6.66495×10^{-5}	0.695743	1.25798	2415.93	2.21331	0.9850

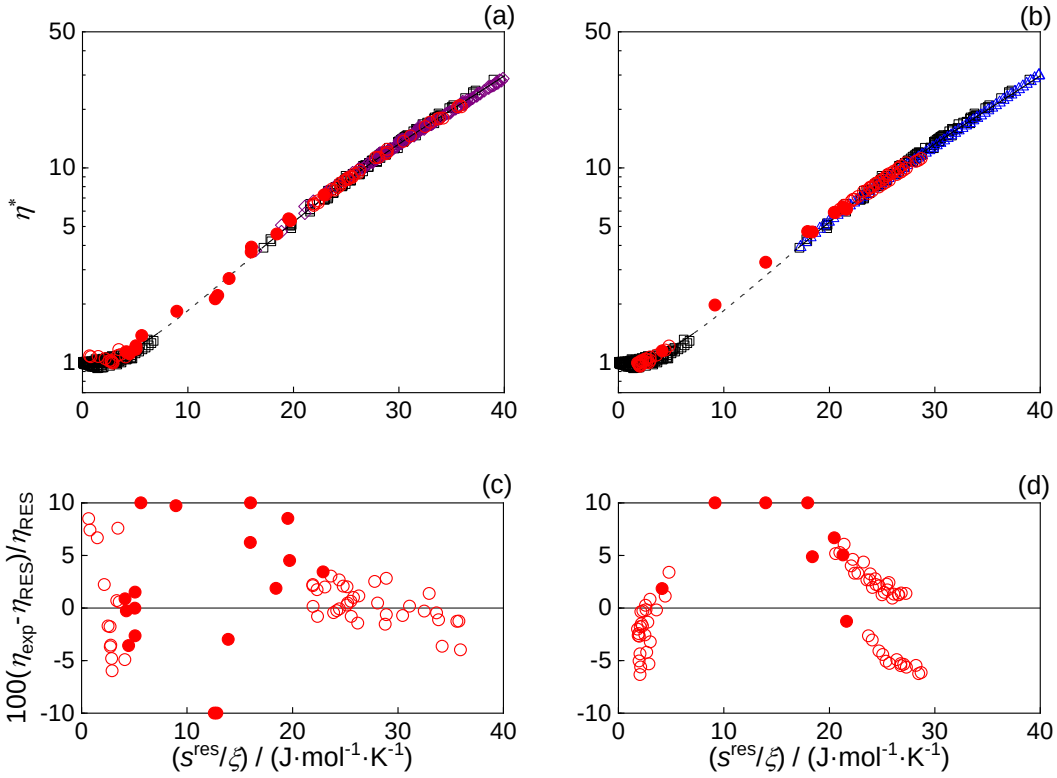

Figure 7. (a) and (b), reduced viscosity η^* *vs* residual entropy s^{res}/ξ for the binary systems of R32 + R1234yf and R32 + R1243zf, respectively. (c) and (d), relative deviation of the experimental viscosities η_{exp} from values η_{RES} calculated with the RES-CPA model *vs* residual entropy s^{res}/ξ for

R32 + R1234yf and R32 + R1243zf, respectively. Symbols: □ R32, ◇R1234yf, △R1243zf, ●: mixture data outside the calculation range (calculation range: not in the vicinity of the critical point) of the RES-CPA model; ○ mixture data within the calculation range of the RES-CPA model.

5. Conclusion

Viscosity measurements of six binary mixtures (R32 + R1234yf and R32 + R1243zf) with R32 mole fraction 0.25, 0.50 and 0.75, respectively, were carried out in the homogeneous liquid and gas phases with a vibrating-wire viscometer in the temperature range from (254 to 383) K at pressures (1 to 8) MPa. The verification measurement was conducted with pure CO_2 and R32 in both liquid and gas phases. The relative combined expanded uncertainties (k = 2) in the experimental viscosity of the mixtures are generally from 3.2 % to 5.0 %, while those near the critical point are up to 7.5 %. The measured viscosities agree with the calculations of the ECS (extended corresponding state) model implemented in the software package REFPROP 10.0 within 10% and mainly within 5%. The relative deviations of the experimental values of R32 + R1234yf mixtures from the ECS model are within the scatter of the literature data. The parameters of the RES-CPA model (residual entropy scaling law incorporating cubic-plus-association equation of state) for the viscosity of R1243zf was determined. The relative deviation of the measured viscosities from values calculated with the RES-CPA model is mainly within 6% in the liquid phase and 10% in the gas phase.

Acknowledgments

The authors are grateful to Prof. Eric F. May of the University of Western Australia in providing part of the facility for carrying out the measurements. The authors are grateful to the National Natural Science Foundation of China [Grant No. 51736005].

References

Al Ghafri, S.Z.S., Rowland, D., Akhfash, M., Arami-Niya, A., Khamphasith, M., Xiao, X., Tsuji, T., Tanaka, Y., Seiki, Y., May, E.F., 2019. Thermodynamic properties of hydrofluoroolefin (R1234yf and R1234ze (E)) refrigerant mixtures: Density, vapour-liquid equilibrium, and heat capacity data and modelling. Int. J. Refrig. 98, 249-260.

Bell, I.H., 2019. Probing the link between residual entropy and viscosity of molecular fluids and model potentials. Proc. Natl. Acad. Sci. U.S.A. 116, 4070-4079.

Bell, I.H., 2020. Entropy Scaling of Viscosity—I: A Case Study of Propane. J. Chem. Eng. Data 65, 3203–3215.
Brown, J.S., Di Nicola, G., Fedele, L., Bobbo, S., Zilio, C., 2013. Saturated pressure measurements of 3, 3, 3-trifluoroprop-1-ene (R1243zf) for reduced temperatures ranging from 0.62 to 0.98. Fluid Phase Equilib. 351, 48-52.
Calm, J.M., 2008. The next generation of refrigerants–Historical review, considerations, and outlook. Int. J. Refrig. 31, 1123-1133.
Chichester, J.C., Huber, M.L., 2008. Documentation and assessment of the transport property model for mixtures implemented in NIST REFPROP (Version 8.0). National Institute of Standards and Technology.
Cui, J., Bi, S., Meng, X., Wu, J., 2016. Surface tension and liquid viscosity of R32+ R1234yf and R32+ R1234ze. J. Chem. Eng. Data 61, 950-957.
Czubinski, F.F., Al Ghafri, S.Z.S., Hughes, T.J., Stanwix, P.L., May, E.F., 2018. Viscosity of a [xCH4+(1− x) C3H8] mixture with x= 0.8888 at temperatures between (203 and 424) K and pressures between (2 and 31) MPa. Fuel 225, 563-572.
Dang, Y., Kamiaka, T., Dang, C., Hihara, E., 2015a. Liquid viscosity of low-GWP refrigerant mixtures (R32+ R1234yf) and (R125+ R1234yf). J. Chem. Thermodyn. 89, 183-188.
Dang, Y., Kim, H.S., Dang, C., Hihara, E., 2015b. Measurement of vapor viscosity of R1234yf and its binary mixtures with R32, R125. Int. J. Refrig. 58, 131-136.
Di Nicola, G., Brown, J.S., Fedele, L., Securo, M., Bobbo, S., Zilio, C., 2013. Subcooled liquid density measurements and PvT measurements in the vapor phase for 3, 3, 3-trifluoroprop-1-ene (R1243zf). Int. J. Refrig. 36, 2209-2215.
Frenkel, M., Chirico, R.D., Diky, V., Yan, X., Dong, Q., Muzny, C., 2005. ThermoData Engine (TDE): software implementation of the dynamic data evaluation concept. J. Chem. Inf. Model. 45, 816-838.
Higashi, Y., Sakoda, N., 2018. Measurements of PvT properties, saturated densities, and critical parameters for 3, 3, 3-trifluoropropene (HFO1243zf). J. Chem. Eng. Data 63, 3818-3822.
Higashi, Y., Sakoda, N., Islam, M.A., Takata, Y., Koyama, S., Akasaka, R., 2018. Measurements of saturation pressures for trifluoroethene (R1123) and 3, 3, 3-trifluoropropene (R1243zf). J. Chem. Eng. Data 63, 417-421.
Huber, M.L., Laesecke, A., Perkins, R.A., 2003. Model for the viscosity and thermal conductivity of refrigerants, including a new correlation for the viscosity of R134a. Ind. Eng. Chem. Res. 42, 3163-3178.
ISO/IEC Guide 98-3, International Organization for Standardization, Geneva, 2008. Uncertainty of measurement - Part 3: Guide to the expression of uncertainty in measurement (GUM:1995).
Laesecke, A., Muzny, C.D., 2017. Reference correlation for the viscosity of carbon dioxide. J. Phys. Chem. Ref. Data 46, 013107.
Lemmon, E.W., Bell, I.H., Huber, M.L., McLinden, M.O., 2018. NIST Standard Reference Database 23: Reference Fluid Thermodynamic and Transport Properties-REFPROP, Version 10.0, National Institute of Standards and Technology. 2018. URL http://www. nist. gov/srd/nist23. cfm.
Liu, H., Yang, F., Yang, Z., Duan, Y., 2020. Modeling the viscosity of hydrofluorocarbons, hydrofluoroolefins and their binary mixtures using residual entropy scaling and cubic-plus-association equation of state. J. Mol. Liq., 113027.

Locke, C.R., Fang, D., Stanwix, P.L., Hughes, T.J., Xiao, G., Johns, M.L., Goodwin, A.R.H., Marsh, K.N., May, E.F., 2015a. Viscosity and Dew Point Measurements of {x CH4+(1–x) C4H10} for x= 0.9484 with a Vibrating-Wire Viscometer. J. Chem. Eng. Data 60, 3688-3695.

Locke, C.R., Stanwix, P.L., Hughes, T.J., Johns, M.L., Goodwin, A.R.H., Marsh, K.N., Galliero, G., May, E.F., 2015b. Viscosity of {xCO2+(1− x) CH4} with x= 0.5174 for temperatures between (229 and 348) K and pressures between (1 and 32) MPa. J. Chem. Thermodyn. 87, 162-167.

Locke, C.R., Stanwix, P.L., Hughes, T.J., Kisselev, A., Goodwin, A.R.H., Marsh, K.N., May, E.F., 2014. Improved methods for gas mixture viscometry using a vibrating wire clamped at both ends. J. Chem. Eng. Data 59, 1619-1628.

McLinden, M.O., Kazakov, A.F., Brown, J.S., Domanski, P.A., 2014. A thermodynamic analysis of refrigerants: Possibilities and tradeoffs for Low-GWP refrigerants. Int. J. Refrig. 38, 80-92.

Myhre, G., Shindell, D., Pongratz, J., 2014. Anthropogenic and natural radiative forcing.

Outcalt, S.L., McLinden, M.O., 1995. Equations of state for the thermodynamic properties of R32 (difluoromethane) and R125 (pentafluoroethane). Int. J. Thermophys. 16, 79-89.

Pal, A., Uddin, K., Thu, K., Saha, B.B., 2018. Environmental assessment and characteristics of next generation refrigerants. Kyushu University.

Span, R., Wagner, W., 1996. A new equation of state for carbon dioxide covering the fluid region from the triple-point temperature to 1100 K at pressures up to 800 MPa. J. Phys. Chem. Ref. Data 25, 1509-1596.

Stanwix, P.L., Locke, C.R., Hughes, T.J., Johns, M.L., Goodwin, A.R.H., Marsh, K.N., May, E.F., 2014. Viscosity of {x CH4+(1–x) C3H8} with x= 0.949 for Temperatures between (200 and 423) K and Pressures between (10 and 31) MPa. J. Chem. Eng. Data 60, 118-123.

Taib, M.B.M., Trusler, J.P.M., 2020. Residual entropy model for predicting the viscosities of dense fluid mixtures. J. Chem. Phys. 152, 164104.

Yang, F., Chu, Q., Liu, Q., Duan, Y., Yang, Z., 2019. The cubic-plus-association equation of state for hydrofluorocarbons, hydrofluoroolefins, and their binary mixtures. Chem. Eng. Sci. 209, 115182.

Yang, X., Arami-Niya, A., Xiao, X., Kim, D., Al Ghafri, S.Z.S., Tsuji, T., Tanaka, Y., Seiki, Y., May, E.F., 2020. Viscosity Measurements of Binary and Multicomponent Refrigerant Mixtures Containing HFC-32, HFC-125, HFC-134a, HFO-1234yf, and CO2. J. Chem. Eng. Data 65, 4252–4262.

Zilio, C., Brown, J.S., Schiochet, G., Cavallini, A., 2011. The refrigerant R1234yf in air conditioning systems. Energy 36, 6110-6120.

Graphical abstract

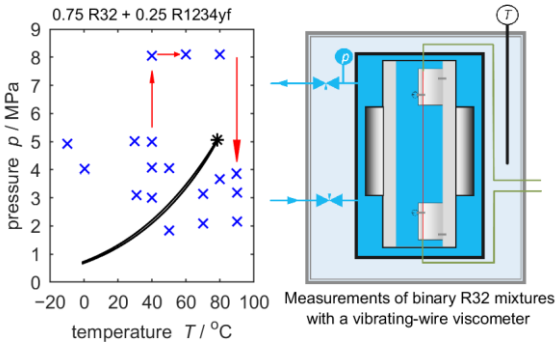
0.75 R32 + 0.25 R1234yf
pressure p / MPa
temperature T / °C
Measurements of binary R32 mixtures
with a vibrating-wire viscometer